Numerical evaluation of indoor thermal comfort and energy saving by operating the heating panel radiator at different flow strategies

Embaye, Mebrahtu; Al-Dadah, Raya; Mahmoud, Saad

DOI:
10.1016/j.enbuild.2015.12.042

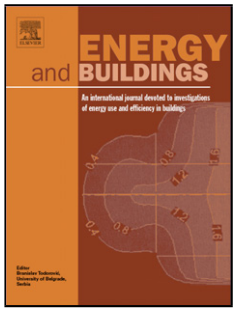

Title: Numerical evaluation of indoor thermal comfort and energy saving by operating the heating panel radiator at different flow strategies

Author: M. Embaye R.K. AL-Dadah S. Mahmoud

PII: S0378-7788(15)30478-3
DOI: http://dx.doi.org/doi:10.1016/j.enbuild.2015.12.042
Reference: ENB 6360

To appear in: *ENB*

Received date: 21-7-2015
Revised date: 21-12-2015
Accepted date: 23-12-2015

Please cite this article as: M. Embaye, R.K. AL-Dadah, S. Mahmoud, Numerical evaluation of indoor thermal comfort and energy saving by operating the heating panel radiator at different flow strategies, *Energy and Buildings* (2016), http://dx.doi.org/10.1016/j.enbuild.2015.12.042

Numerical evaluation of indoor thermal comfort and energy saving by operating the heating panel radiator at different flow strategies

M. Embaye, R. K. AL - Dadah, S. Mahmoud
School of Mechanical Engineering, University Of Birmingham

ABSTRACT

Enhancing the performance of central heating systems in buildings can play a major role in energy savings. Pulsed flow to the radiators can lead to enhancing the specific heat output of radiators. The aim of this work is to investigate the effect of radiator flow pulsation on the indoor spatial temperature and velocity distributions to achieve energy saving without compromising the user thermal comfort defined by ASHRAE standard 55 and EN ISO 7730. CFD modelling of panel radiators at constant and pulsed flows were carried out and the results were validated with published data. Such radiators were then incorporated in a room and CFD modelling of the room was carried out using flow pulsation strategies.

The simulation of the radiator at constant flow was validated against published experimental data in terms of heat output showing maximum deviation of 2.44%. Results from CFD simulation of the radiator with pulsed flow using frequency ranging from 0.0083Hz to 0.033Hz and amplitude ranges from 0.0168kg/s to 0.0228kg/s showed that 25% improvement in the specific heat output can be achieved while maintaining the same radiator target surface temperature of 50^{o}C. Also using the pulsed flow applied in this work the pump power can be reduced by about 12% compared to the pump operating at constant flow. As for the heated space with the integrated radiator, results of CFD simulation for pulsed flow with frequency of 0.033Hz and amplitude of 0.0192kg/s showed that the temperature, velocity and draught rate were maintained within the required comfort levels of 20±1.5^{o}C; less than 0.15m/s and less than 15% respectively.

- CFD simulation of hydronic panel radiators and heated rooms with constant and pulsed flow conditions
- Flow pulsation enhances the heat transfer performance of hydronic panel radiators
- Pulsating the flow of hydronic radiator increases specific heat output of panel radiators that by 25%
- The work highlights the potential of energy saving using flow pulsation for panel radiator while maintaining the indoor comfort standards of the occupants

Key words: Indoor comfort, Specific energy output, CFD, Heat transfer, Pulsed flow

Nomenclature

Symbols

A	Area [m^2]
F	Volume force [N/m^3]
d_h	Hydraulic diameter [m]
DR	Draught risk [%]
f	Frequency [Hz]
g	Gravity [m/s^2]

HTER Heat Transfer Enhancement Ration (%)
C_p Specific heat capacity [J/(kg.K)]
L Characteristics length [m]
LMTD log mean temperature difference [K]
$\dot{m}$ Mass flow rate [kg/s]
P Pressure [Pa]
PD Percentage of Dissatisfied [%]
PED Percentage Experience Draught [%]
Per Perimeter [m]
Q Heat energy [W]
Sp.Q Specific heat capacity [kW/Kg]
Re Reynolds number [-]
St Strouhal number [-]
T Temperature [K]
t Time [s]
TI Turbulent Intensities [%]
U Average velocity [m/s]
V Velocity [m/s]

Greek symbols

ρ Density [kg/m^3]
α Thermal conductivity [w/(m.K)]
v Kinetic viscosity [m^2/sec]
μ Dynamic viscosity [N s/m^2]

Subscripts

out Outlet/Output
in Inlet/Inflow
PF Pulsed flow
CF Constant flow
rad radiator
ind indoor

1. INTRODUCTION

Published energy consumption data indicate that around 50% of the total energy consumption is used for buildings in developed countries [1]. For example, in the UK buildings services consume 40% of the overall energy consumption, thus contributing about half of the UK's CO_2 and other environmental pollutants emissions which contribute to global warming [2]. To meet the 20% energy reduction target by 2020, the UK is aiming to reduce residential buildings energy consumption by 52% [3]. Enhancing the efficiency of domestic central heating system without affecting the wellbeing/comfort of the occupants is an important factor in achieving the considered reduction target [4]. Various research works have been published regarding enhancing the performance of such system and the user indoor comfort phenomena. *Figure 1*

describes the closed loop panel radiator hydronic heating system showing the heat source, panel radiator and the space to be heated. The parameters used to assess the comfort of occupants in air conditioned space include indoor temperature (T_{ind}), indoor air velocity (V_{ind}), Percentage Dissatisfied (PD), Percentage Experienced Draught (PED) and Draught Risk [DR] [5].

According to ASHRAE standards 55 maintaining indoor comfort phenomena is key objective when one attempt to reduce the heat energy consumption of buildings integrated with central heating system. Various research papers have been reported regarding the indoor comfort parameter including temperature, velocity, PD, DR and PED. The indoor comfort was investigated under ventilated hydronic radiator as a heat source in a room with Swedish standard of ventilating air flow of 0.0086kg/s per person using CFD. Results showed that ventilated radiators are able to create more stable thermal comfort climate than the traditional radiators [6]. An office room was investigated numerically at high, medium and low temperature radiator surface as well as floor heating to investigate the indoor comfort including air speed, cold draught and temperature. And it was conclude that, room installed with low temperature radiators can offer lower indoor temperature fluctuations which lead to low energy consumption and better occupants comfort [7]. Kana et al. investigated the effect of wall thickness in thermal energy consumption and indoor comfort of the occupants [8]. They concluded that the thermal loss of thin wall (20cm) is 53% higher compared to thicker wall (40cm) while having the same heat transfer coefficient, also indoor comfort temperature of thinner wall is 4.6^{o}C lower compared to the thicker walls. Therefore it was concluded that indoor comfort and thermal energy loss can be affected by thermal conductivity variation of the walls. Ge et al. study to investigate the cause of cold indoor draught due to extreme cold outdoor temperature combined with poor glazing transmittance [9]. They recommended that the cold draught comfort problem can be improved using well insulated glazing. Arslan and Kose also conducted thermoelectric optimization on the insulation thickness in building [10]. Bhaskoro et al. conducted CFD simulation of heated space with two radiators as a heat sources and virtual sitting of manikin in the room to investigate the occupant comfort parameters [11]. They concluded that properly insulated external walls and windows glazing create stable indoor comfort and low energy consumption in the air conditioned room.

Smart control management of central heating system can also play important role to reduce energy consumption and improve the comfort temperature of the occupants [12]. Artificial neural network (ANN) based predictive and adaptive logic control also has a potential for indoor comfort control by decreasing the standard deviation of indoor temperature range, decreasing percentage of overshoots and undershoots of the desired indoor comfort ranges [13]. Embaye et al. investigated the indoor comfort temperature using PID control system compared to the on/off control system and concluded that using PID control system can create better indoor stability with lower indoor fluctuations of ±1^{o}C and lower energy consumption of the building to be heated [14].

There are various heat transfer enhancement methods including: rough surfaces; nanofluids; fluid slipping enhancers, surface coating, fin attachments, mechanical mixing device, vibration, magnetic electric fields and flow pulsation [15-18]. Flow pulsation was used to enhance heat transfer in various industrial applications including heat exchangers, pulse combustors, electronic cooling devices, cooling system of nuclear reactors leading to a potential of reducing energy consumption by up to 60% [19-23]. Embaye et al. investigated the effect of flow pulsation on the energy consumption of heating radiators [24] and concluded that up to 20% of energy saving can be achieved by pulsation the flow with 0.033Hz frequencies and 0.0228kg/s amplitudes. However they didn't investigate the effect of flow pulsation of heated radiator on the thermal comfort of heated space. Thus the presented work aims to investigate numerically (CFD) the effect of flow pulsation in a hydronic central heating radiator on the thermal comfort of occupants compared to the conventional constant flow one.

2. RADIATOR AND HEATED SPACE CONFIGURATION

Figure 2 shows the dimension and mesh density of the simulated panel radiator with top-bottom opposite end (TBOE) connections and *Table 1* shows its thermal properties. This radiator includes rectangular ducts with 15mm width and 1mm thickness, metal fins with thickness of 0.5mm and hot water as a working fluid [25 and 26]. The radiator model was meshed based on the geometrical structure of each component; swept rectangular mesh was generated for the fins (478080 elements numbers) and tetrahedral mesh was selected for the water domain and the flow channels (1759121 element numbers). The simulation period using computer specification of Intel(R) Core (TM) i7-3770 CPU @ 3.40GHz; memory (RAM) 16GB and 64-bit operating system is about 28hrs for the panel radiator standalone and 72 hours for the heated room (radiator integrated in the room to be heated). Also the simulation time step was set to 30s.

The dimensions of the heated space were selected as a single person office with controlled ventilation as a fresh air source and hydronic heating radiator as a heat source. *Table 2* shows the thermal properties of all materials used to construct the heated space. *Figure 3* shows the dimension and mesh distribution for the heated space model. It includes the panel radiator, window, internal walls, external walls, ceiling, roofs and air volume [27]. A tetrahedral mesh of 200937 elements was generated for the heated space.

3. CFD SIMULATION METHODOLOGY

In this study the thermal performance of a heated space using hydronic radiator was simulated using COMSOL multiphysics software [28]. COMSOL is a finite element analysis, simulation, and solver software package for numerous physics and engineering applications, including coupled heat transfer and fluid flow analysis. The transient simulation of the integrated radiator and room system proved to be very demanding in computational time. Therefore, the 3D finned

heating radiator is simulated separately with its surface temperature predicted and compared to published data. Then, the transient radiator surface temperature was used in the simulation of the heated space to predict the spatial temperature distribution, air velocity, draught ratings and energy saving. *Figure 4* shows the flow chart of the CFD simulation process.

The CFD simulations were carried out using conjugate heat transfer physics module in COMSOL. The k-ε turbulence model was used to predict the flow pattern for both the radiator and the room. This model has been reported to be more robust than other turbulence models [26, 29]. The governing equations used to carry out the simulations are conservation of momentum eq. (1); conservation of continuity eq. (2); conservation of energy eq. (3); turbulence kinetic energy rate eq. (4); turbulence dissipation rate eq. (5) and turbulent kinetic pressure eq. (6).

$$\rho\frac{\partial u}{\partial t}+\rho(u.\nabla)u=\nabla.[-pI+(\mu+\mu_T)*(\nabla u+(\nabla u)^T)-\frac{2}{3}(\mu+u_T)(\nabla.u)I-\frac{2}{3}\rho\kappa I]+F \quad (1)$$

Where; $\mu_T=\rho C_\mu\frac{\kappa^2}{\varepsilon}$

$$\frac{\partial\rho}{\partial t}+\nabla.(\rho V)=0 \quad (2)$$

$$\rho C_p\frac{dT}{dt}+\rho C_p V.\nabla T=\nabla.(\alpha\nabla T)+Qs \quad (3)$$

$$\rho\frac{\partial\kappa}{\partial t}+\rho(u.\nabla)\kappa=\nabla[(\mu+\frac{\mu_T}{\sigma_\kappa})\nabla\kappa]+p_\kappa-\rho\varepsilon \quad (4)$$

$$\rho\frac{\partial\varepsilon}{\partial t}+\rho(u.\nabla)\varepsilon=\nabla[(\mu+\frac{\mu_T}{\sigma_\varepsilon})\nabla\varepsilon 1]+C_{\varepsilon 1}\frac{\varepsilon}{\kappa}p_\kappa-C_{\varepsilon 2}\rho\frac{\varepsilon^2}{\kappa} \quad (5)$$

$$p_\kappa=\mu_T[\nabla u:(\nabla u+(\nabla u)^T)-\frac{2}{3}(\nabla.u)^2]-\frac{2}{3}\rho\kappa\nabla.u \quad (6)$$

Where: u, Qs, I, ε, μ_T, α, V, F, and κ are; vector velocity, heat source other than viscous, identity matrix of [3*3], turbulence dissipation rate, turbulence dynamic viscosity, heat conductivity, volume, volume force and the turbulence kinetic energy respectively.

For modelling the panel radiator, the following assumptions were used:

- Natural convection cooling was applied on the air side surface of the radiator at ambient temperature of 20°C.
- Constant hot water inlet supply temperature of 75°C was applied for radiator as recommended in the BS EN-442 radiator standards testing.
- Heat transfer due to radiation was applied at constant emissivity value 0.85.

As for the heated space modelling, the following assumptions were used:

- There was no water flow in the radiator model, instead transient temperature profile obtained from the simulated hyronic radiator was applied on the surface of the radiator inside the heated room
- The room was assumed to be empty; all heat gains from the sun, light bulbs, other equipment were neglected the only heat source was the panel radiator surface temperature profile.

4. CFD RESULTS OF CONSTANT FLOW RADIATOR

The single finned panel radiator (type11 shown in *Figure 2*) is numerically simulated at constant hot water inlet volume flow rate 0.0119kg/s. Simulation results were validated using experimental data reported by [27, 28 and 29] who used EN-442 radiator standards testing method in their work. *Figure 5* shows the local surface temperature distribution (a); the variation of mean temperature of radiator eq.(7), LMTD eq.(8), and water outlet temperature with time (b) at the operating conditions of 0.0119 kg/s hot water flow rate, hot water inlet temperature of 74.76^{o}C and ambient temperature of 19.89^{o}C [29 and 30]. *Table 3* compares the predicted and experimental values for the output parameters including the radiator mean temperature the hot water outlet temperature and LMTD. The deviation between the predicted and experimental results is calculated using eq. (9).

$$T_{mean} = \frac{T_{rad,\ in} + T_{rad,\ out}}{2} \tag{7}$$

$$LMTD = \frac{T_{rad,\ in} - T_{rad,\ out}}{ln\left(\frac{T_{rad,\ in} - T_{ind}}{T_{rad,\ out} - T_{ind}}\right)} \tag{8}$$

$$\text{Diff}\ \ \% = \left|\frac{Exp - CFD}{\text{Exp}}\right| * 100 \tag{9}$$

It is clear from *Table 3* that the maximum deviation between the predicted and experimental results is 2.44% for the radiator heat output indicating the validity of the numerical simulation results.

4.1 CFD RESULTS OF HEATED ROOM AT CONSTAN FLOW

All thermal comfort assessment is undertaken after the space reaches equilibrium indoor temperature at 2000s. The room simulation was carried out using inlet air ventilation at a rate of 0.6 air changes/h, average ambient winter temperature of 5^{o}C and initial indoor

temperature of 20°C. Convection cooling boundary condition was considered for window and external walls; surface to surface radiation was considered between the panel radiator and the radiator side wall at emissivity of 0.9. All other walls were applied as adiabatic boundary conditions and all material properties for the room were taken from *Table 2*. The natural convection of the heated room air volume is applied using buoyancy driven volume force expressed in eq. (10). This buoyancy force will affect both the air within the room and the fresh air entering the room due to ventilation. The fresh air was defined based on the number of inlet air changes and had a temperature equal to the ambient.

$$F = -g.(\Delta\rho) \tag{10}$$

In buoyancy driven volume force heat transfer occurs due to the density difference of the indoor air (natural convection).

The predicted mean surface temperature of the constant flow radiator was fitted using a polynomial equation as shown in eq. (11) and used as a boundary condition for the heated space transient model shown in figure 5 as T_mean radiator.

$$T_{mean,Cf} = (t <= 500) * (9^{-7} * t^3 - 0.001 * t^2 + 0.3562 * t + 320.15) + (t > 500) * (342.3) \tag{11}$$

Where: $T_{mean,Cf}$ is the mean temperature distribution profile generated from surface panel radiator simulated under constant flow case and t is the time. The radiator is achieving its thermal equilibrium at a controlled scenario by selecting the hot water flow rate to the radiator according to of BS EN-442 radiator standard testing.

Figure 6 shows local temperature distribution and indoor velocity of the heated room indicating that the local indoor temperature and air velocity distributions are within the recommended limits of 20±2°C and 0.15 m/s respectively according EN ISO 7730 comfort standards.

5. CFD RESULTS OF PULSED FLOW RADIATOR

The thermal boundary condition of the pulsed flow radiator model is the same as the constant flow; the only difference is the inlet hot water flow which is pulsating. The flow was pulsated at various flow velocity amplitudes as shown in *Table 4* and *Figure7*, with Strouhal number (defined in eqn. (12)) ranging from 0.23 to 0.65; and Reynolds number (eqn. (13)) ranging from 0 to 1838.

$$St = \frac{f.L}{U} \tag{12}$$

$$\mathrm{Re} = \frac{U.d_h}{\nu} \tag{13}$$

Where: $d_h = \frac{4.A}{2Per}$

Figure 8 shows the radiator specific heat output (defined by eqn. (14)) at various amplitude ranging from 0.0168kg/s to 0.0228kg/s with constant frequency of 0.033Hz and various frequencies ranging from 0.0083Hz to 0.033Hz with constant flow amplitude of 0.0192kg/s. Figure 8(a) shows that the flow amplitude of 0.0192kg/s gave the highest specific heat output while Figure 8 (b) shows that the flow frequency that achieved highest specific heat output was 0.033Hz.

$$Sp.Q = \frac{Q_{output}}{\dot{m}_{input}} \tag{14}$$

As shown in *Figure 8*; the best pulsed flow specific heat output was obtained at flow velocity amplitudes of 0.0192kg/s and frequency of 0.033Hz. *Figure 9* shows the local surface temperature distribution; mean temperature of radiator eq. (7), LMTD eq. (8), and outlet hot water temperature of the best pulsed flow radiator.

5.1 ENERGY SAVING DUE TO PULSED FLOW

Energy saving due to the pulsed flow compared to the constant flow is estimated using the specific heat transfer rate of the radiator eq. (14) and *Figure 10* (a). The percentage of instantaneous and average Heat Transfer Enhancement Ratio (HTER) is estimated using eq. (15) and *Figure 10* (b). The operating scenario that gives high specific heat output rate and higher percentage of heat transfer enhancement indicates the best heat output performance of the simulated radiators.

$$HTER = \left(\frac{Sp.Q \quad Pulsed \ \ flow}{Sp.Q \ \ Constant \ flow} - 1 \right) \times 100 \tag{15}$$

The improvement in the specific heat output is related to the average supply mass flow rate required to achieve the target LMTD of 50^{o}C of simulated heating radiator. The shaded areas in Figure 10 (a) represent the 25% improvement in the specific heat output of the hydronic radiator due to flow pulsation compared to the constant flow. The heat transfer enhancement achieved by pulsed flow is attributed to the increase of the Reynolds number and flow vertices around boundary layers that leads to higher flow disturbance in the radiators flow channels.

The power consumption of the central heating system consists of the thermal energy consumption associated with the boiler and the electrical energy consumption (mainly from the circulation pump). The 25% improvement in the specific heat output from the radiator related to thermal energy consumption from the boiler.

As for the pump electrical energy consumption, it was not considered due to being small (around 6% of the total energy consumed [31]) compared to the thermal energy consumption. However, using the pulsed flow applied in this work the pump power consumption was calculated analytically using equations provided in [15] and showed that a reduction of about 12% compared to the pump operating at constant flow can be achieved. This is because the amplification of pump power at the peak of the pulse flow is compensated by the off time period of the pulsed flow as shown in figure 7.

5.2 CFD RESULTS OF HEATED ROOM AT PULSED FLOW

The heated room at radiator pulsed flow scenario is simulated using the similar boundary condition that of the constant flow heated room expect the heat source (panel radiator) boundary condition. The radiator mean transient surface temperature shown in figure 9 at pulsed flow was fitted by equation (16) and applied as a boundary condition for the simulated heated room at pulsed flow.

$$T_{mean,PF} = (t <= 500) * (9^{-7} * t^3 - 0.001 * t^2 + 0.36 * t + 321.15) + (t > 500) * (343.15 + wv) \quad (16)$$

Where: T_{PF}, t, and wv are the temperature (K) distribution profile generated from surface panel radiator simulated under pulsed flow, time (s) and sine wave function respectively.

Figure 11 shows the local indoor temperature and air velocity distribution in the heated room at 2000s indicating that they are within the recommended human comfort targets of $20^{o}C \pm 2^{o}C$ and 0.15(m/s) respectively. The temperature is lower around the bottom of the room which is expected; also the air velocity distributions are lower at the bottom of the room that shows downdraught air at the ankle level is supressed. Thus results of room CFD model under pulsed flow is well counteracting to the fresh cold air coming from outdoor due to ventilation. When

the flow is pulsed the room reaches thermal equilibrium (steady state) by 10% faster than the constant flow case thus the flow control has positive impact on the indoor thermal comfort by improving the thermal inertia.

6. Indoor comfort analysis

6.1 Indoor temperature and velocity validation

According to ASHRAE 55 standards the recommended occupants indoor comfort margin is considered from 0.1m (ankle level) to 1.1m above the floor level for person sitting in office and 0.1m to 1.7m for standing person. All trends are taken at 2000s when the heated room reaches thermal equilibrium. The recommended indoor comfort temperature and indoor air velocity $20\pm2^{o}C$ and $\leq$ 0.15 m/s respectively. The presented simulated CFD results for both constant flow and pulsed flow cases of the room models where fully able to overcome the heat demand as well as distribute the temperature and velocity evenly throughout the whole room. The air velocity at the ankle level is below 0.1m/s increasing upwards to the ceiling reaching a maximum of 0.14 m/s and the indoor temperature remains at range of $20.5^{o}C$ to $21.5^{o}C$ in the desired occupied zone. Figure 12 shows the indoor air velocity and temperature profile at specified vertical position of the simulated room compared to the experimentally validated work found in [18]. As shown in Figure 12 (a) and Figure12 (b) the trend are taken at vertical centre of the simulated room x, y, Δz values of 2.4m, 1.2m 2.66m respectively. Also the second trends shown in Figure 12 (c) and Figure 12 (d) are taken at 1m away from the surface of wall surrounding the room x, y, Δz value of 3.8m, 1.2m, 2.66m respectively. The temperature and velocity profile of simulated room models are in a good agreement with validated data found in literature and indoor comfort standards of EN ISO 7730 as well as with recommended indoor comfort standards of temperature and velocity.

6.2 Indoor draught ratings

The discomfort due to draught in a ventilated room is estimated by Draught Risk (DR) parameters which depend on the local turbulence intensity (TI) of the room in percent and it expressed in eq. (17) [27, 28 and 32]. The prediction Percentage of Dissatisfied (PD) due to draught expressed by eq. (18) refer to people who are exposed to indoor air velocity in the occupied zone with turbulence intensity ranging 35 to 55% under sedentary conditions. There is also other important mathematical equation that help to predict the Percentage Experience Draught (PED) a sedentary occupant of the ventilated room expressed using eq. (19). The three draught prediction equations are included in both ASHRAE standard 55 and EN ISO 7730 indoor comfort zone standards also the turbulence intensity (TI) is expressed using eq. (20).

$$DR = \left[(3.143 + 0.3696 * V_{in,air} .TI).(34 - T_{in,air})*(V_{in,air} - 0.05)^{0.6223}\right] \quad (17)$$

$$PD = 13.8*10^{3}.\left[\left(\frac{V_{in,air} - 0.04}{T_{in,air} - 13.7} + 2.93*10^{-2}\right)^{2} - 8.54*10^{-4}\right] \quad (18)$$

$$PED = 113*(V_{in,air} - 0.05) - 2.15*T_{in.air} + 46 \quad (19)$$

$$TI = \frac{V'}{U} \quad (20)$$

Where; V' is Root-Mean-Square (RMS) of the turbulent velocity fluctuations at a particular location over a specified period of time, U is the average of the velocity at the same location over same time period [32, 33].

Figure 13 shows the draught discomfort condition of the CFD simulated rooms under constant flow and pulsed flow compared to validated data found in literature [18] at thermal equilibrium of the heated room. Figure 13 (a),(b) and (c) shows the DR, PED and PD in % at ankle level of 0.1m horizontally along the width of the room (y-axis) and at coordinates values of x, Δy , z are 1.5m, 2.36m , 0.1m respectively. Figure 13 (d), (e), (f) shows the DR, PED and PD in % at ankle level of 0.1m horizontally along width of the room y-axis and values of x, Δy , z are 3.8, 2.36m , 0.1m respectively. As shown in figure 13 all the comfort parameters related to draught ratings are in a good agreement with validated data as well as with internationally recommended draught ratings percentage of $\leq$ 15%.

7. CONCLUSIONS

Achieving energy saving without compromising thermal comfort of building occupants is prominent importance. This work investigates through CFD simulation the thermal comfort parameters of heated space with constant and pulsed flow of hydronic panel radiator central heating system. ALL CFD simulations for this work were performed using conjugate heat transfer (CHT) in COMSOL Multiphysics. CFD model of radiator was developed and numerically simulated using constant flow and pulse flow cases. The radiator at constant flow was validated with experimental work and the results were in good agreement with maximum deviation of 2.44%. Results from the panel radiator showed that 25% improvement in the specific heat output can be achieved with pulsed flow due to higher heat transfer rate compared to conventional constant flow. About 12% of pump power consumption (electrical) saving was also possible due to the pulsed flow compared to the constant flow.

The transient mean temperature profile of the simulated radiator was fitted and used in simulating the heated room for both constant and pulsed flow operating scenarios. Results of the room models showed that the comfort parameters that achieved indoor comfort at temperature of 20±1.5^{o}C, indoor velocity below 0.15m/s and the draught rating parameters are all (PD, PED, DR) below 15%. All comfort criteria presented in this work are achieved as

recommended by the international comfort standards of ASHRAE 55 and EN ISO 7730. Results of the simulated room are compared with validated data found in literature and a good agreement is achieved without any significant deviation that compromises the wellbeing of the room occupants. Also the pulsed flow gives a 10% faster indoor comfort temperature response by improving the thermal inertia. Thus this work highlights the potential of energy saving due to the improvement in the specific heat output using flow pulsation for panel radiator while maintaining the indoor comfort standards of the occupants.

8. REFERENCES

[1] Z. Fang, N. Li, G. Luo, Y. Huang. The effect of building envelope insulation on cooling energy consumption in summe. Energy and Buildings 2014; 77:197-2005.

[2] http://www.ukgbc.org/content/key-statistics-0 [accessed 20/08/2014]

[3] D. Dineen, B.P. Ó. Gallachóir Modelling the impacts of building regulations and a property bubble on residential space and water heating. J. Energ Buildings. 2011; 43: 166-178.

[4] G. Kim, L. Schaefer, T. S. Lim, J. T. Kima. Thermal comfort prediction of an underfloor air distribution system in a large indoor environment. Energy and Buildings 2013; 64: 323–331.

[5] A. Ploskic, S. Holmberg. Heat emission from skirting boards. Building and Environment 2010. 1123-1133.

[6] M. A. John, S. Halberg. Design Consideration with ventilation-radiators comparisons to traditional two-panel radiators. Energy and buildings 2009; 41: 92-100.

[7] J. A. Myhren; S. Holmberg. Flow patterns and thermal comfort in a room with panel, floor and wall heating. Energy and Buildings 2009, 41:92-100.

[8] H. Kana, Y. Yufeng, Y. Jun. Modelling conjugate flow and heat transfer in a ventilated room for indoor thermal comfort assessment. Building and Environment 2014; 77:135-147.

[9] H. Ge, P. Fazio. Experimental investigation of cold draft induced by two different types of glazing panels in metal curtain walls. Journal of Building and Environment 2004;39: 115–25.

[10] O. Arslan, R. Kose. Thermo economic optimization of insulation thickness considering condensed vapour in buildings. Energy and Buildings 2006; 38:1400–1408.

[11] P. T. Bhaskoro, I. Syed, M. S. Aris. Numerical analysis of air flow, heat transfer, moisture transport and thermal comfort in a room heated by two-panel radiators. Energy and Buildings 2011; 43:137–146.

[12] Yu Chen Jingye Zhao. Applications of the Strong Heat Transformation by Pulse Flow in the Shell and Tube Heat Exchange. ICEBO. 2006; Shenzhen, 11-105.

[13] J. W. Moona,1, J.H. Lee, S. Kimc. Application of control logic for optimum indoor thermal environment in buildings with double skin envelope systems. Energy and Buildings 2014; 85:59-71.

[14] M. Embaye, R.K. AL-Dadah, and S. Mahmoud. Effect of flow pulsation on energy consumption of a radiator in a centrally heated building. International Journal of Low-Carbon Technologies 201; 0: 1-11.

[15] engineeringtoolbox.com [accessed on 12/10/2014].

[16] S.M.B. Beck, S.C. Grinsted, S.G. Blakey, K. Worden. Novel design for panel radiators. Journal of applied Thermal Energy 2004; 24: 1291–1300.

[17] A. Ploskic, S. Holmberg. Low temperature baseboard heaters with integrated air supply analytical and numerical investigations. Energy and Environment 2011; 46: 176-186.

[18] A. Ploskic, S. Holmberg. Heat emission from thermal skirting boards. Building and Environment 2010; 45:1123–1133.

[19 A.R.A. Khaled. Heat transfer enhancement due to properly managing the distribution of the heat flux. Energy Conversion and Management 2012; 53:247-258.

[20] G. Li, Y. Zheng, G. Hu, Z. Zhang. Experimental investigation on heat transfer enhancement from an inclined heated cylinder with constant heat input power in infrasonic pulsating flows. ETF. 2013.

[21] H.N. Hamida, M.N. Sabry, A. Abdel-Rahim, H. Mansour. Theoritical analysis of heat transfer in laminar pulsating flow. IJ of heat and mass transfer 2002; 45: 1767-1780.

[22] D.J. Sailor, D. J. Rohli, Q. Fu. Effect of variable duty cycle flow pulsations on heat transfer enhancement for an impinging air jet. Heat and fluid flow 1999; 20: 574-580.

[23] J. Gustafsson, J. Delsing, D. Jan van. Improved district heating substation efficiency with a new control strategy. J. Appl. Energy 2010; 87: 1996 - 2004.

[24] M. Jafari, M. Farhad, K. Sedighi. Pulsating flow effects on convection heat transfer in corrugated channel. Heat and Mass transfer 2013; 45:146-154.

[25] M. Embaye, R.K. AL-Dadah, S. Mahmoud. Thermal performance of hydronic radiator with flow pulsation – Numerical investigation. Applied Thermal Engineering, April 2015; 80:109–117.

[26] E. Aydar, I. Ekameci. Thermal efficiency estimation of the panel type radiator with CFD analysis. Thermal science and Technology 2012; 32: 63-71.

[27] The Harmonisation of Thermal Properties of Building Materials:http://www.esru.strath.ac.uk/Documents/89/thermop_rep.pdf [accessed 30/09/2014].

[28] COMSOL Multiphysics version 4.3.

[29] A. Berkan. Simulation of the heater test room defined by EN442 standard and virtual testing of different type of heaters (PhD thesis). 2011.

[30] Comparative thermal performance of test on two reflective panels forms radiators. BSRIA April 2003.

[31] https://www.plumbnation.co.uk/site/boilers/?manufacturer=worcester&page=1 [[accessed 25/10/2014].

[32] Z. Vlahostergios, D.Missirlis, M.Flouros, C. Albanakis, K.Ykinthos. Effect of turbulence intensity on the pressure drop and heat transfer in a staggered tube bundle heat exchanger. Experimental Thermal and Fluid Science 2014; 60: 75-82.

[33] J. R. D. Dear, G.S. Brager. Thermal comfort in naturally ventilated buildings: revisions to ASHRAE Standard 55. Energy and Buildings 2002; 34:549-561.

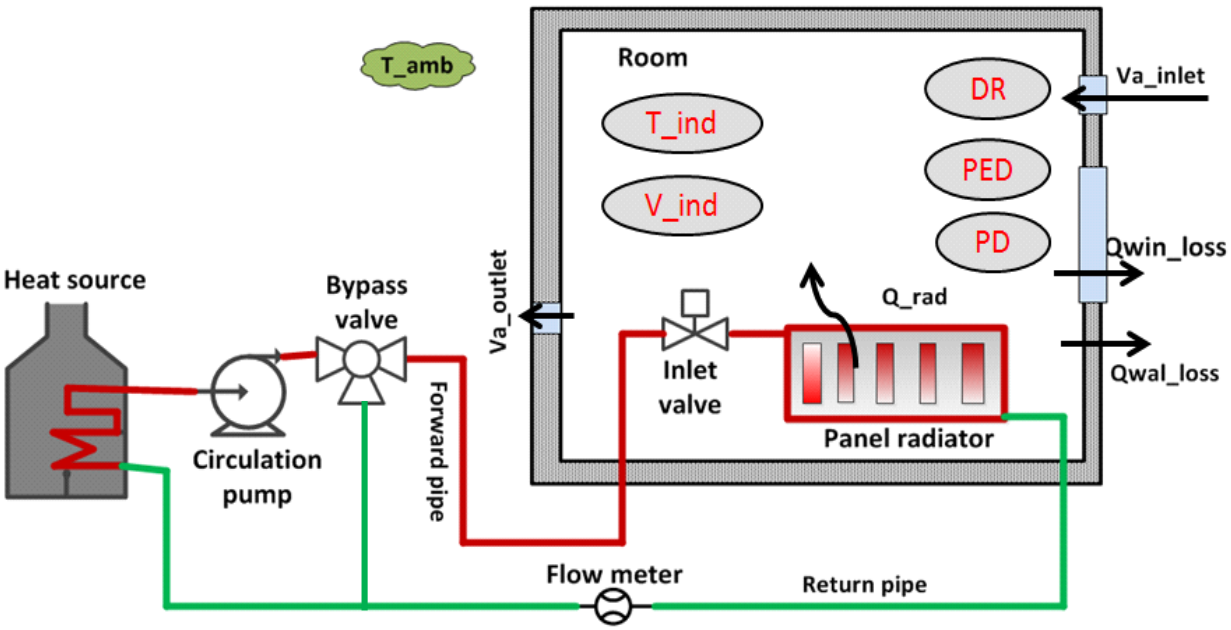

Figure 1 closed loop hydronic central heating system layout

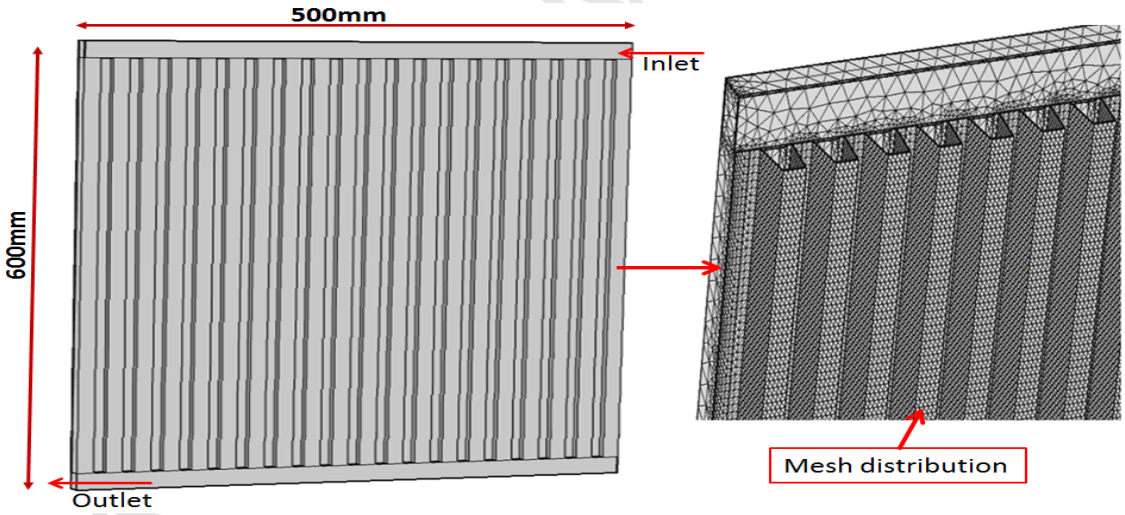

Figure 2 dimension and mesh distributions of the panel radiator

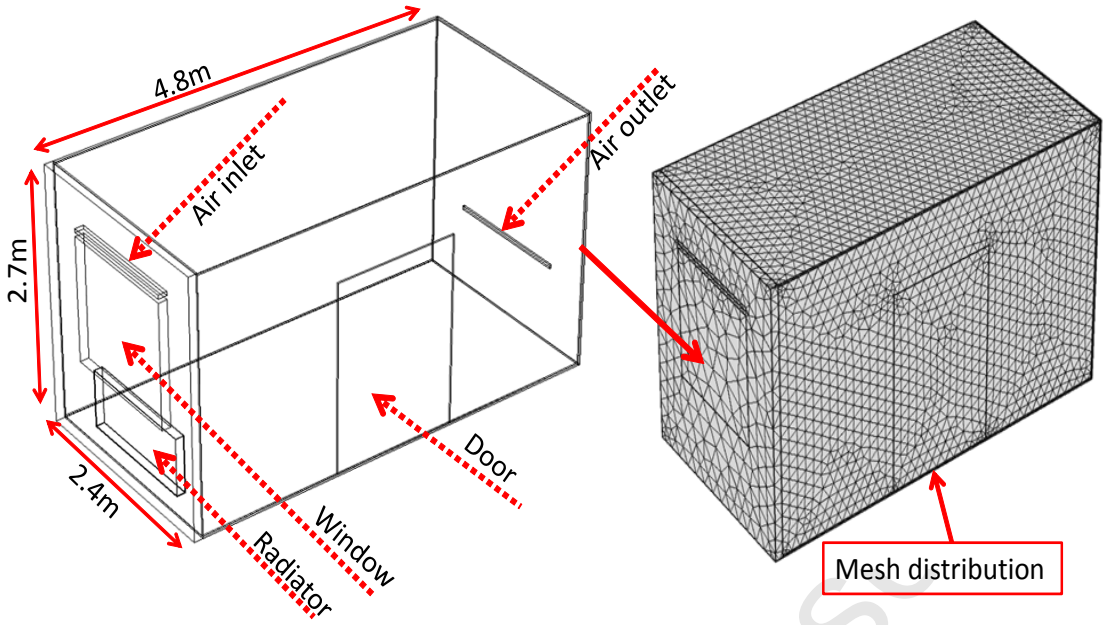

Figure 3 the CAD design dimension and mesh distribution of the room model

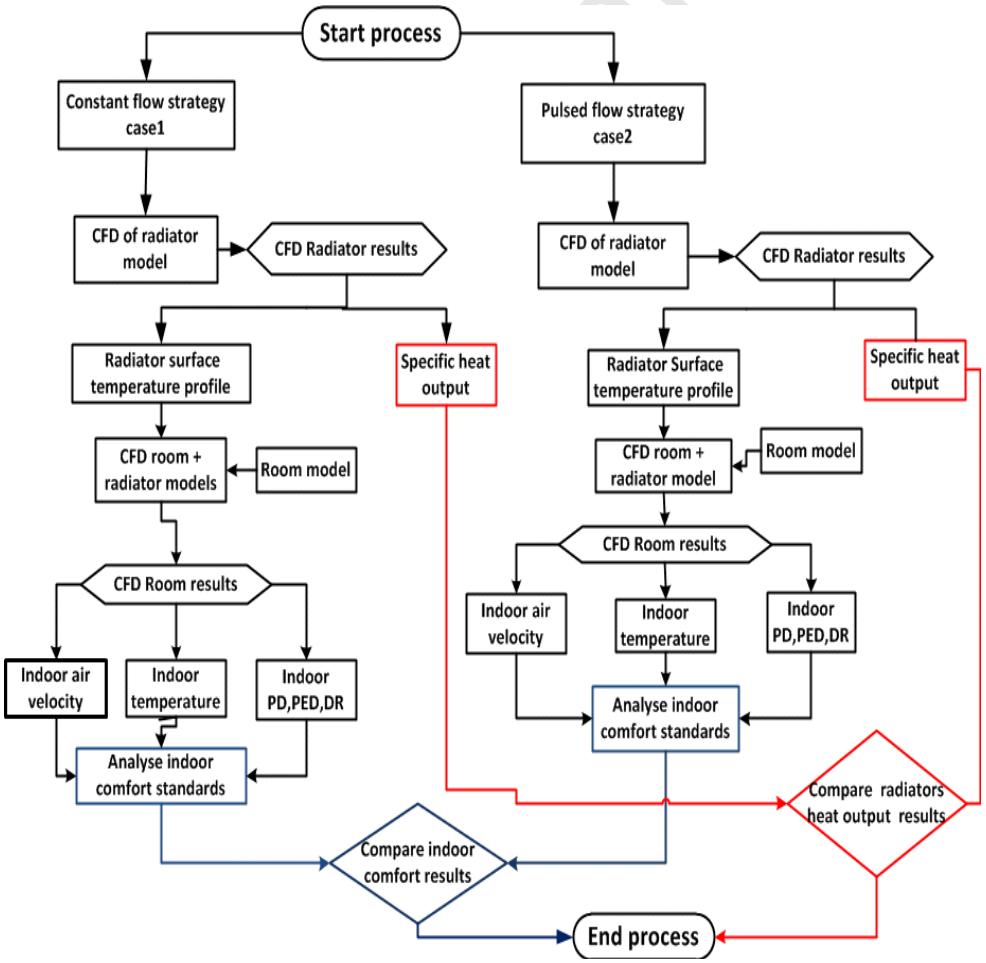

Figure 4 flow diagram of CFD simulation process

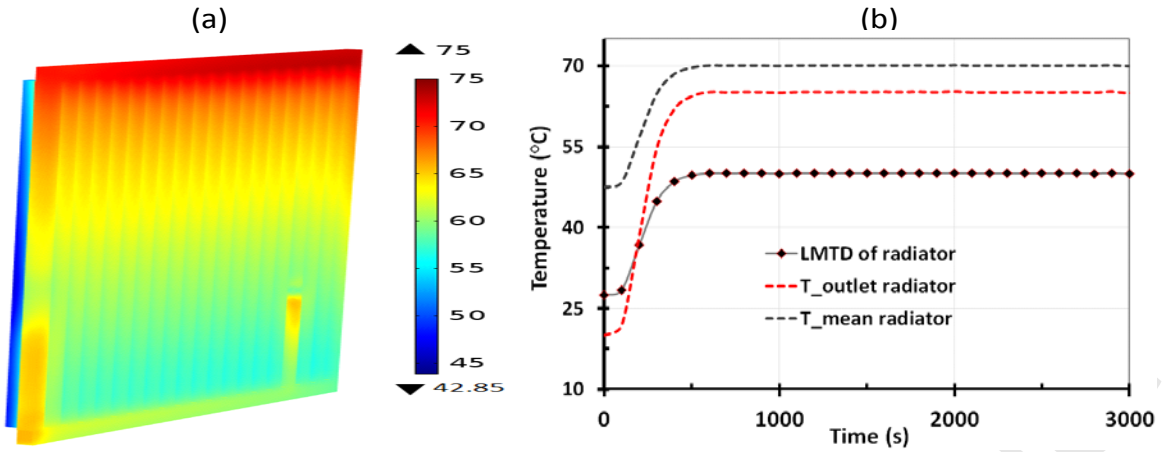

Figure 5 (a) contour of local surface temperature distribution (^{o}C); (b) LMTD, hot water output temperature and specific heat energy of the constant flow radiator

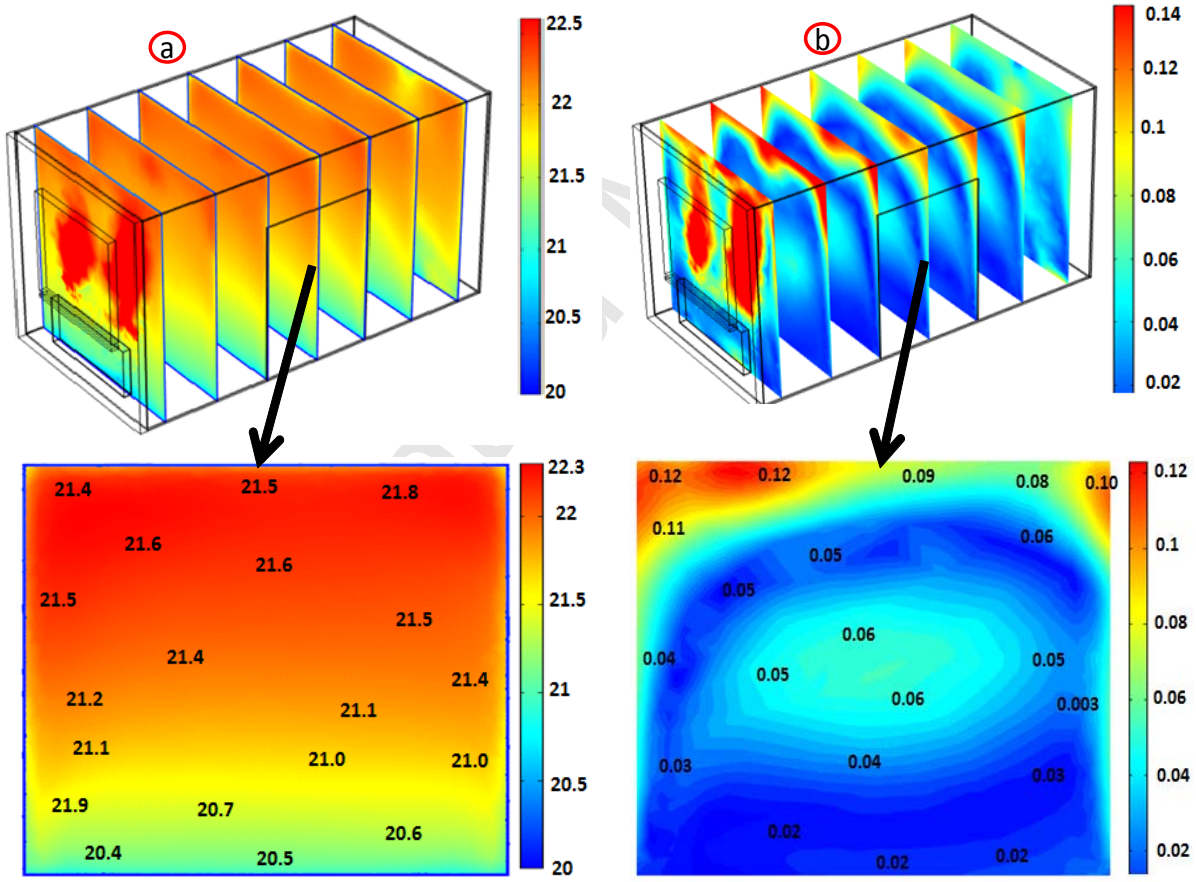

*Figure 6 (**a**) Slice (top left) and contours vertical centre plane (bottom left) of local temperature [^{o}C] of the room. (**b**) Slice (top right) vertical centre plane (bottom right) of the indoor velocity for the constant flow case at 2000s*

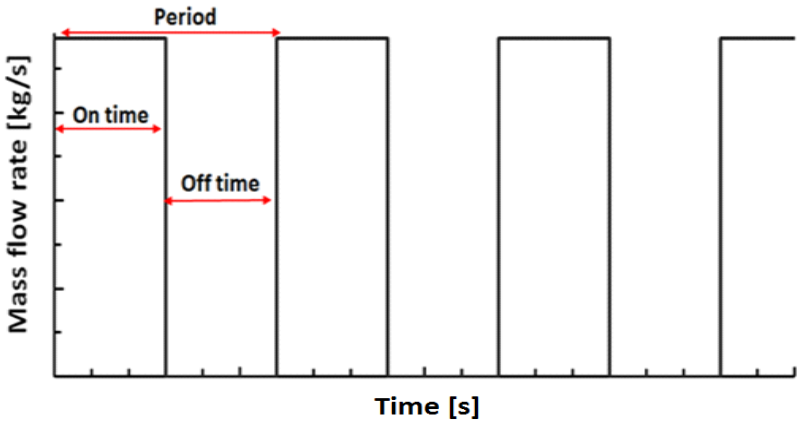

Figure 7 Pulsed flow velocity input profile

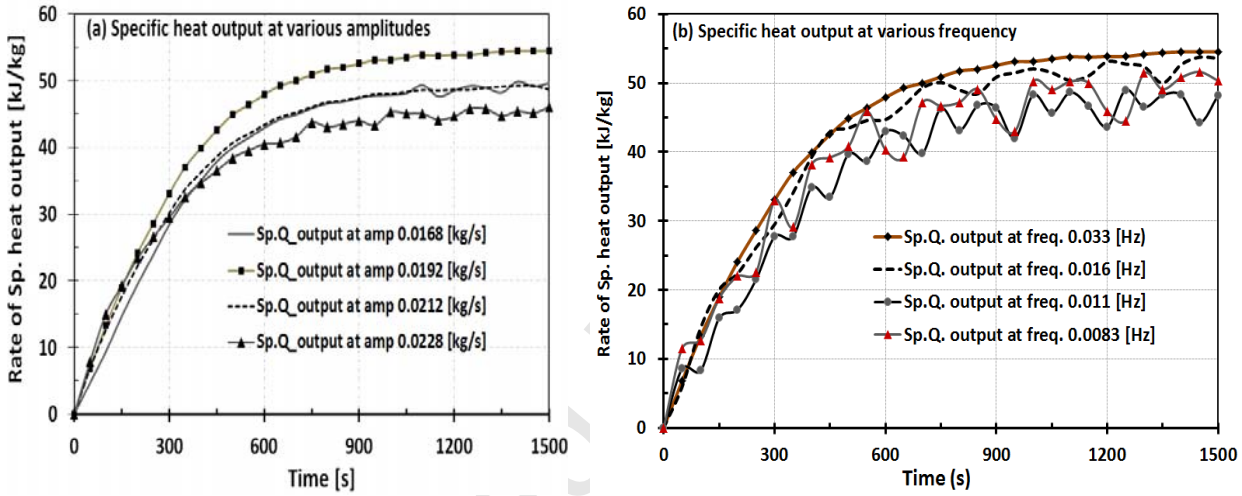

Figure 8 (a) specific heat output at various amplitudes but constant freq. of 0.033Hz (b) specific heat output at various frequencies but constant amps 0.0192kg/s

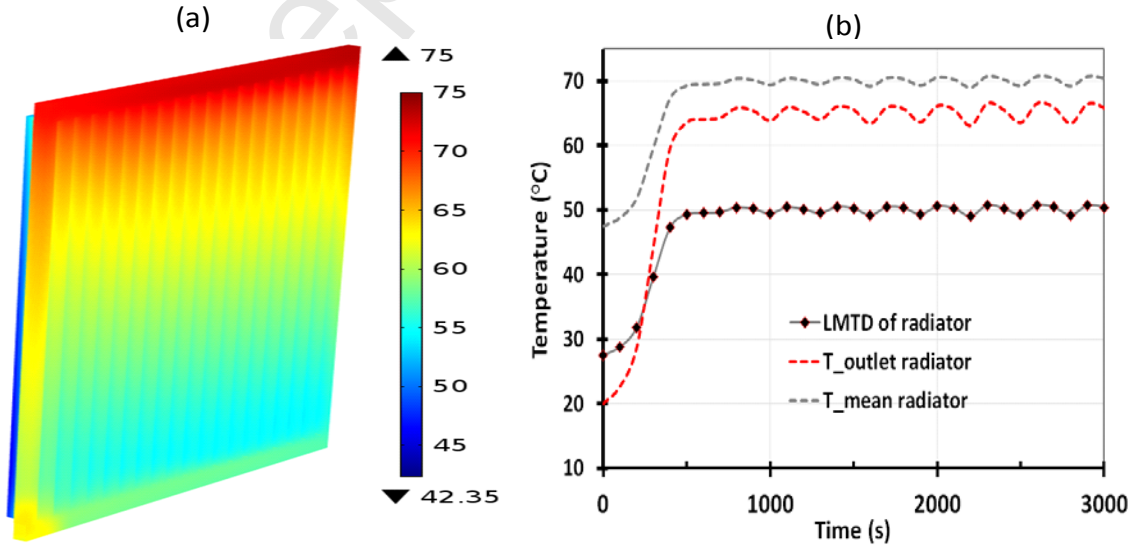

Figure 9 Contour of local surface temperature distribution (oC); average surface temperature; hot water output temperature and heat output of proposed pulsed flow radiator (case2) at the selected amplitudes of 0.0192kg/s

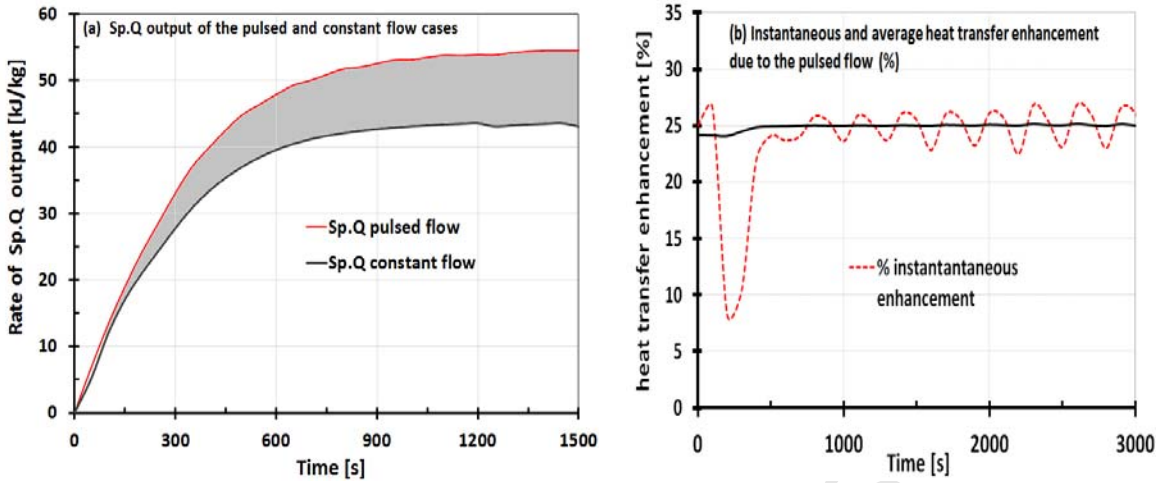

Figure 10 (a) Specific heat capacity of the radiators simulated at constant flow and pulsed flow (b) heat transfer enhancement of the radiator due the pulsed flow

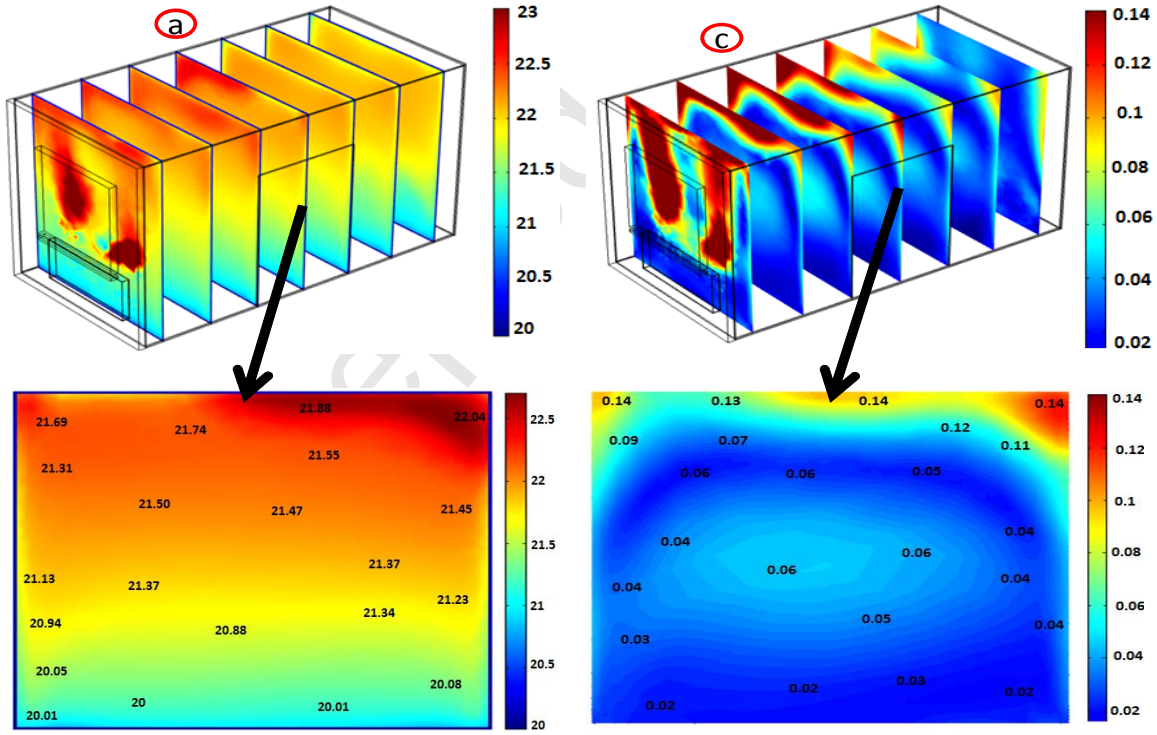

*Figure 11 (**a**) Slice (top left) and contours vertical centre plane (bottom left) of local temperature of the room. (**b**) Slice (top right) vertical centre plane (bottom right) of the indoor velocity for the pulsed flow at 2000s*

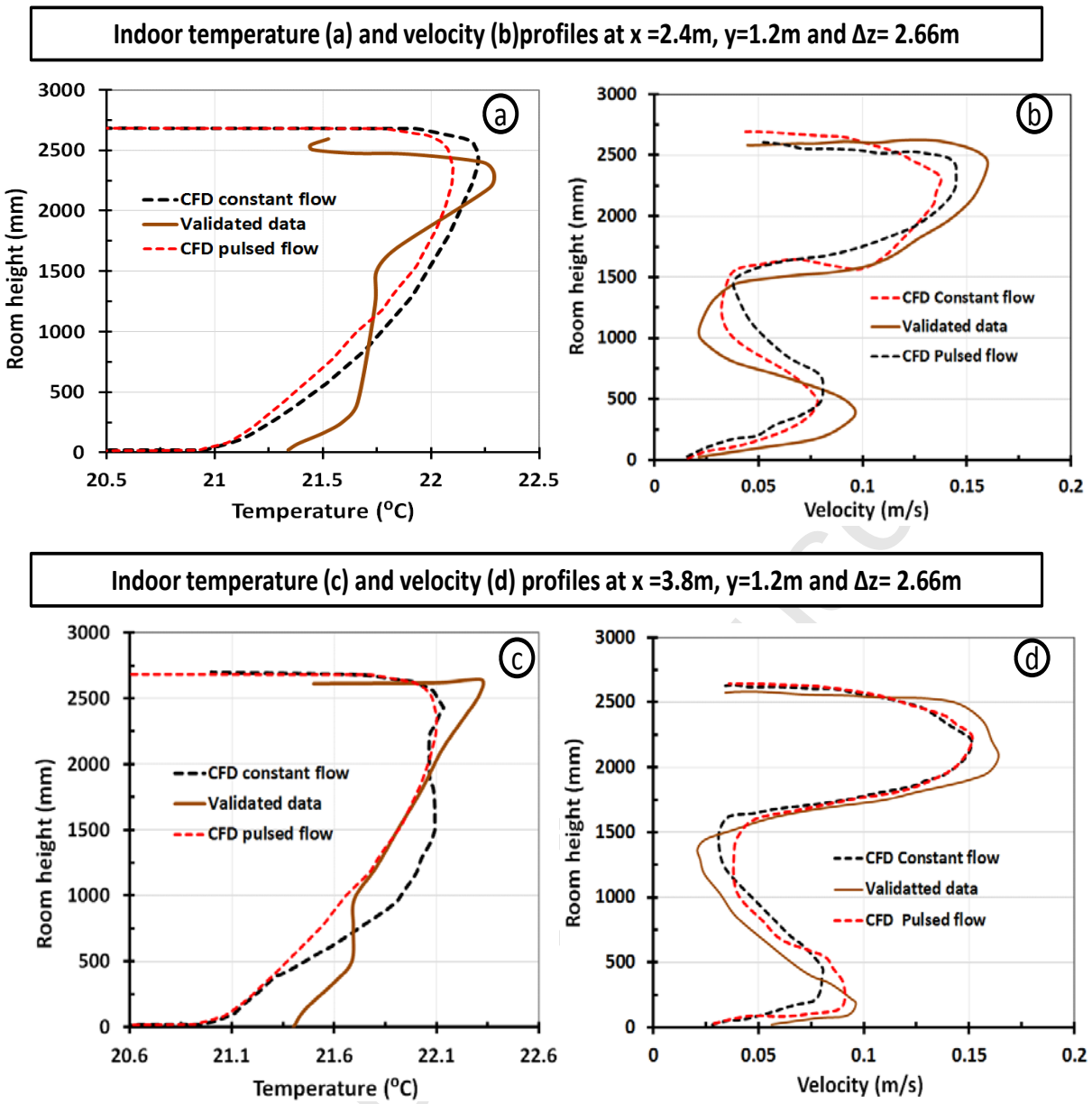

Figure12 Temperature and velocity profile of the CFD room models compared to validated data from literature at 2000s

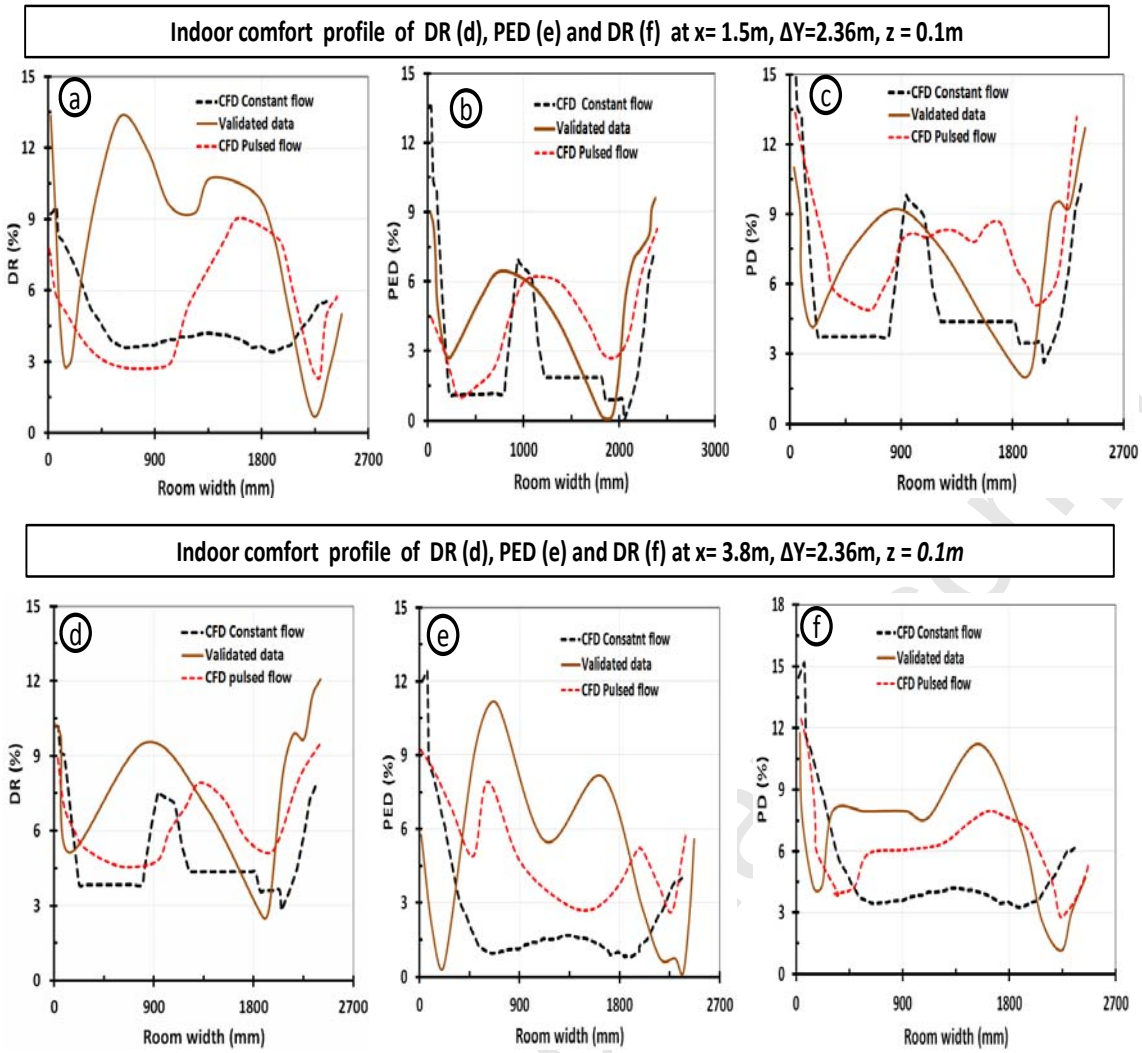

Figure13 Comfort description of the indoor room in respect to EN ISO 7730 standards the CFD room models validated against experimental data at 2000s

Table1 thermal properties for the for radiator model

Domain type	Materials type	K [W/m.K]	$C_{p,}$ [J/kg.K]	ρ [kg/m^3]
Fluid	Water	0.58	4180	1000
Channels	Steel	16.5	475	7850
Fins	Steel	16.5	475	7850

Table2 thermal properties of room model materials

Components	Materials	K [W/m.K]	c [J/kg.K]	ρ [kg/m^3]
Internal wall	Bricks	0.84	600	1700
External wall	Bricks	0.62	800	1700
Window and door	Glass	0.96	600	2200
Floor and Ceiling	Wood	0.42	842	1200
Radiator	Steel	16.5	475	7850
indoor	Air	0.025	1005	1.2
Door	wood	0.14	1200	650

Table 3 CFD results and experimental (literature) results of the single fined panel radiator [29]

Specifications	CFD	Exp	Diff %
Flow rate (kg/s)	0.023	0.023	
Ambient temperature (^{o}C)	19.98	19.98	
Inlet temperature (^{o}C)	74.76	74.76	
Outlet temperature (^{o}C)	64.83	64.71	0.15
Mean temperature (^{o}C)	69.79	69.76	0.043
Log Mean Temperature Difference (K)	49.15	49.76	1.20
Radiator heat output (W)	992.1	968.42	2.44

Table 4 Pulsed flow amplitudes at constant frequency of 0.209 rad/s

Radiator pulsed flow inlet	
Amplitudes [kg/s]	Average mass (kg/s]
0.0168	0.0084
0.0192	0.0096
0.0215	0.0107
0.0228	0.0114